Tina Memo No. 2011-009
Internal

Estimating Anisotropic Measurement Errors on Landmarks; Extension from 2D to 3D.

Hossein Ragheb, Neil.A.Thacker.

Last updated
10 / 12 / 2011

Imaging Science and Biomedical Engineering Division,
Medical School, University of Manchester,
Stopford Building, Oxford Road,
Manchester, M13 9PT.

Estimating Anisotropic Measurement Errors on Landmarks; Extension from 2D to 3D.

Abstract

Our intention is to utilise the statistical methods we have developed, for analysis of shape data with anisotropic measurement covariances, as a tool to monitor manual and automatic placement of landmarks. We wish to make quantitative assessments of measurement accuracy, and also identify potential errors in mark-up at the level of $\leq 5\%$ of the data sample. This document outlines the mechanism we have used to extend 2D shape rotation analysis, and the extraction of corrected anisotropic measurement covariances (Tina Memo 2010-009), to 3D. The methods are demonstrated in the analysis of 3D mouse mandible data, both as a test of the theory/software implementation and as an illustration of use for the identification of outlier landmarks.

Introduction

The extension to 3D data is mainly involved with the mechanism of representing and estimating 3D shape rotations. We define a fixed orientation co-ordinate system from a set of 3D data-points based upon a selection of three landmark points. We then represent a rotation matrix in terms of three separate rotations about the co-ordinate axes. Finally we compute the linear vectors which approximate the first order shifts seen in the 3D points due to these rotations. These are then used in the linearised approximation for sample covariance correction, as described in previous work. These extensions are enough to support a quantitative analysis of 3D landmark data, for the estimation of landmark accuracy and identification of outlier data. The mathematical model used is described in detail in the following sections and followed by quantitative tests which demonstrate the numerical stability of the algorithms using Monte-Carlo data.

Rotation Matrix

Our first task is to define a co-ordinate system for a 3D data-set, from which we can define certain basic properties of orientation for the mean shape, and so that individual data samples can be approximately oriented prior to optimisation during linear model construction. In the 2D case this is done by simply defining the line between two landmark points in the mean model as horizontal. In 3D this situation is more complicated as we have the possibility of a rotation matrix which must be defined by a minimum of 3 parameters. In order to stay consistent with the 2D case we define 2 points to establish a horizontal, and then a third to define the vertical relative to the first two.

Given a 3D shape, take three points p_1, p_2, p_3, with relatively large distance from each other, to define the orientation plane for the shape (Fig. 1).

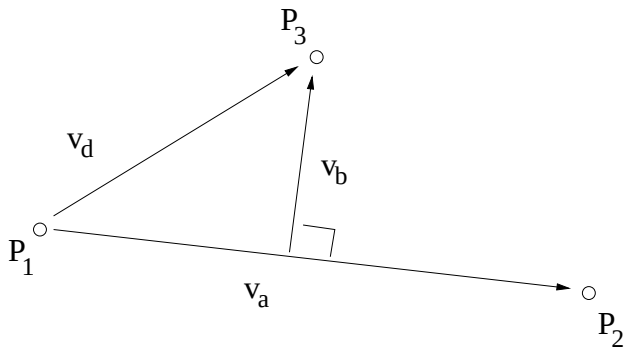

Figure 1:

Find the rotation matrix R based on basic vector calculations as follows.

$$\hat{v}_a = \frac{p_2 - p_1}{\|p_2 - p_1\|} \tag{1}$$

$$v_b = (p_3 - p_1) - [(p_3 - p1).\hat{v}_a]\hat{v}_a \tag{2}$$

$$\hat{v}_c = \hat{v}_a \times \frac{v_b}{\|v_b\|} \tag{3}$$

$$R^T = \begin{pmatrix} \hat{v}_{ax} & \hat{v}_{ay} & \hat{v}_{az} \\ \hat{v}_{bx} & \hat{v}_{by} & \hat{v}_{bz} \\ \hat{v}_{cx} & \hat{v}_{cy} & \hat{v}_{cz} \end{pmatrix}$$

Roll, Pitch and Yaw Angles

Given the rotation matrix which brings a dataset into alignment with the preferred co-ordinate system it is now possible to represent the rotation as a sequence of rotations about three orthogonal axes. According to basic 3D rotation formulas, and using α, β, and γ as yaw, pitch, and roll respectively, the 3d rotation matrix is defined as three consecutive rotations around the z, y, and x coordinate axes.

$$R^T = R_x(\gamma)R_y(\beta)R_z(\alpha) \tag{4}$$

where

$$R_x(\gamma) = \begin{pmatrix} 1 & 0 & 0 \\ 0 & \cos\gamma & -\sin\gamma \\ 0 & \sin\gamma & \cos\gamma \end{pmatrix}$$

$$R_y(\beta) = \begin{pmatrix} \cos\beta & 0 & \sin\beta \\ 0 & 1 & 0 \\ -\sin\gamma & 0 & \cos\beta \end{pmatrix}$$

$$R_z(\alpha) = \begin{pmatrix} \cos\alpha & -\sin\alpha & 0 \\ \sin\alpha & \cos\alpha & 0 \\ 0 & 0 & 1 \end{pmatrix}$$

and so

$$R_{x-y-z} = \begin{pmatrix} \cos\beta\cos\alpha & -\cos\beta\sin\alpha & \sin\beta \\ \cos\gamma\sin\alpha + \sin\gamma\sin\beta\cos\alpha & \cos\gamma\cos\alpha - \sin\gamma\sin\beta\sin\alpha & -\sin\gamma\cos\beta \\ \sin\gamma\sin\alpha - \cos\gamma\sin\beta\cos\alpha & \sin\gamma\cos\alpha + \cos\gamma\sin\beta\sin\alpha & \cos\gamma\cos\beta \end{pmatrix}$$

By making the rotation matrix R^T equivalent to R_{xyz}, we find the yaw, pitch, and roll angles given by

$$\alpha = -\tan^{-1}(R^T[1][2]/R^T[1][1]) \tag{5}$$
$$\beta = -\sin^{-1}(R^T[1][3]) \tag{6}$$
$$\gamma = -\tan^{-1}(R^T[2][3]/R^T[3][3]) \tag{7}$$

Thus we can convert easily between the rotation matrix and rotation parameters.

Orientation Adjustments

In order to perform shape alignment, we must initialise the rotation angles. This is done by computing the R^T matrix for every original shape in the data set and extracting its corresponding α, β, and γ angles. These are then further adjusted during iterative alignment via optimisation of the an-isotropic measurement based Mahlanobis distance. We also need to perform orientation adjustment on the mean shape following every iteration over the set of shape samples. In this case the set of yaw, pitch, and roll angles from the mean shape are subtracted off the corresponding rotation angles for each shape sample. Following convergence of the model the computed mean shape then complies with the orientation constraint defined according to our three point method.

Direction Vectors

In order to correct the covariances due to alignment parameters, we compute the approximate linear direction vectors corresponding to translation, rotation and scale. Computing these for translation and scale are straightforward.

For rotation, we compute the direction vector corresponding to each individual rotations R_z, R_y and R_x. For the mean shape $\mathbf{m}$ rotated by the yaw angle α around the z axis, we have $\mathbf{m}' = R_z(\alpha)\mathbf{m}$, i.e. at each landmark point with $\mathbf{m}_x$, $\mathbf{m}_y$ and $\mathbf{m}_z$ as the mean coordinates we can write

$$\mathbf{m}' = \begin{pmatrix} \cos\alpha\mathbf{m}_x - \sin\alpha\mathbf{m}_y \\ \sin\alpha\mathbf{m}_x + \cos\alpha\mathbf{m}_y \\ \mathbf{m}_z \end{pmatrix}$$

The direction vector then would be the first derivatives of the vector $\mathbf{m}'$ with respect to the angle of rotation α, as α becomes very small, i.e.

$$\mathbf{u}_\alpha = \begin{pmatrix} -\sin\alpha\mathbf{m}_x - \cos\alpha\mathbf{m}_y \\ \cos\alpha\mathbf{m}_x - \sin\alpha\mathbf{m}_y \\ 0 \end{pmatrix}$$

Hence the tangential direction of movement in landmark points due to this rotation is

$$\mathbf{u}_{\alpha\approx 0} = \begin{pmatrix} -\mathbf{m}_y \\ \mathbf{m}_x \\ 0 \end{pmatrix}$$

This corresponds to the linearised approximation vector which was used previously for correction of anisotropic 2D measurement covariances. By applying the same method, one can find the direction vectors due to rotation by the pitch angle β around the y axis and due to rotation by the roll angle γ around the x axis, i.e.

$$\mathbf{u}_{\beta\approx 0} = \begin{pmatrix} \mathbf{m}_z \\ 0 \\ -\mathbf{m}_x \end{pmatrix}$$

$$\mathbf{u}_{\gamma\approx 0} = \begin{pmatrix} 0 \\ -\mathbf{m}_z \\ \mathbf{m}_y \end{pmatrix}$$

The three direction vectors are mutually orthogonal and orthogonal to the direction vector due to scaling which is $\mathbf{u}_s = [\mathbf{m}_x, \mathbf{m}_y, \mathbf{m}_z]$. These now constitute the linearised parameterisations needed for corrections to the sample covariance for degree of freedom biases.

Experiments

As our method is based on likelihood, we require that the assumed distribution matches the sample covariance (more correctly the bias-corrected covariance). The standard way to validate this is through generating Monte-Carlo (MC) data using the known distributions. Here each shape sample is projected onto the fitted linear model and a new sample generated equivalent based upon this "noise free" shape perturbed with the estimated anisotropic error. This preserves the sample distribution allowing stability issues arising due to distribution anomalies (such as outliers and non-linear distributions) to be identified. For **known linear model parameters**, and sample distributions which match the Gaussian and Linear model assumptions, the covariances used by the Monte-Carlo are expected to be within statistical sampling limits of the ones estimated. Here we use 2.8 standard deviations of the error on the sample variance (equivalent to 1% of data being expected to fall outside the limits), where the error on the standard deviation σ is $\sigma/\sqrt{2(K-1)}$ with K being the number of samples. Additional variance will be seen for the case where the linear model must also be estimated, so that we can interpret variations beyond the statistical limits as due to instability in linear model construction (specifically the mean and eigen vectors). In what follows we experiment with MC data and display a number of informative scatter plots.

We experiment with the Apodemus mouse mandible 3D data of manual mark-ups (provided by our collaborators at Max Planck as a typical 3D data set). The data corresponds to mouse mandible micro-CT images and consists of 87 samples with 20 landmarks per sample. This data has been obtained by averaging each left and right points into one 3D location, in order to eliminate problems with missing data.

As will be shown below, using our Monte-Carlo tests, we found that some outliers exist in the data. Hence, we applied our outlier detection tool to the original data and, based on the list of potential outliers it provides (Table 1), chose to remove two samples (14 and 42) from the input TPS data file. These samples require further investigation in order to determine the cause of this poor conformity to the rest of the data. This leaves 85 samples in the data to experiment with. Although some evidence of outliers remains, the Monte Carlo results indicate that these are no longer present at a level which destabilises estimation of the linear model. We notice that this data (in terms of the biological structures under study) is similar to the 2D mouse mandible data (provided earlier by our collaborators). Hence we chose to use 5 components in the liner model.

sample	landmark	error (standard deviation)
14	7	5.474743
14	8	5.531980
14	9	5.698620
14	10	5.725281
14	11	5.775997
14	12	5.782629
14	13	5.858766
14	14	5.998678
14	15	6.215031
14	16	6.229069
14	17	6.303817
14	18	6.317162
14	19	6.338735
14	20	6.694317
42	14	5.186163
42	15	5.294472
42	16	5.535036
42	17	5.655291
42	18	5.738199
42	19	5.759585
42	20	5.806348
23	16	5.356338
23	17	5.519671
23	18	5.708450
23	19	5.949248
23	20	6.025292

Table 1: Outlier removal: Following analysis and estimation of the anisotropic measurement error, the software lists any landmarks which lie more than a statistical (χ^2) threshold from the fitted linear model. Here we list samples corresponding to the top three largest number of errors over the allowable threshold (set to 5.0), when our method (5-components model) applied to the original Apodemus data (87×20); we chose to remove only the samples 14 and 42. Further data may be removed until estimates of the eigen vectors (and hence anisotropic measurement error estimate Fig 3.), agree with the Monte-Carlo data generation parameters within the expected statistical limit.

Exp. A: Here when applying our method to the MC data, the mean shape, eigen-vectors and measurement covariances used during analysis are identical to the ones used when generating the simulated data (Figs. 2 and 3). The results indicate that for the original data (Fig. 2) there are some eigen-values falling significantly outside the statistical allowable range. This occurs because the presence of outliers destabilises the estimation of residual variances, even in the case where the Monte-Carlo data has been generated according to the assumed distributions. This further indicates that a linear model cannot be reliably fitted to extract the linear deformation parameters while such data samples are present. In contrast for the data without outliers (Fig. 3) all eigen-values fall within the range expected. These results validate our software implementation and show that this Monte-Carlo test can tell us if there are outliers in the data.

Exp. B: An independent model including mean model and linear eigen-vectors is generated using the MC data in order to compare the distributions of errors estimated using the simulated data against those which are expected, i.e. the ones assumed when generating the MC data (Figs. 4 and 5). In this case, as the model parameters are adjusted to minimise residual error, the effects of outliers (large increases) of eigen values are reduced in comparison to Exp. A. However, the general trend for better predicted eigen-values is still present and the results in Fig. 5 indicate the general level of accuracy of the anisotropic errors expected for real data. The need to fit model parameters destabilises the smaller eigen-values slightly w.r.t. to 1% lower limit computed from sample statistics. These results provide an estimate of the repetability of accuracy of the mark-up process which generated this data.

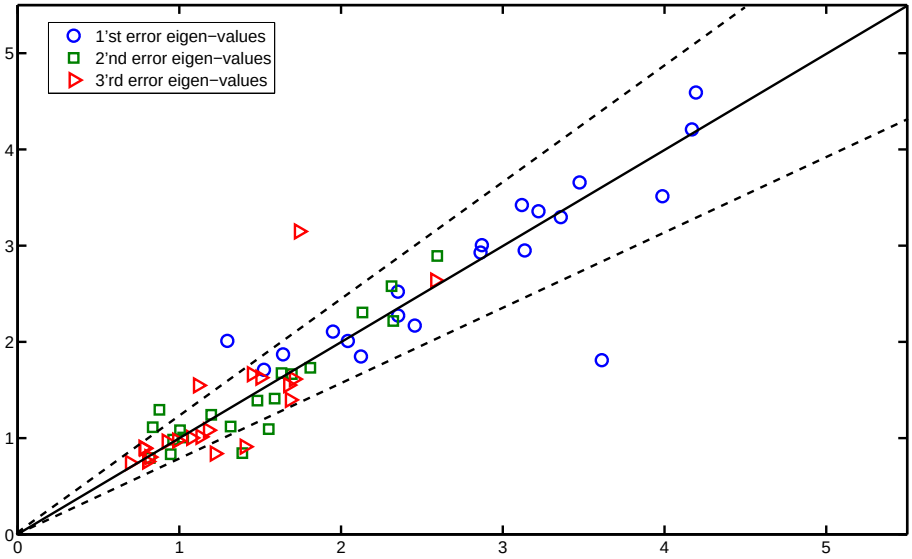

Figure 2: Original Apodemus data (87×20): error eigen-values estimated using the Monte-Carlo data (where mean shape, eigen-vectors, and measurement covariances are identical to the 5-component model which generated the simulated data) against the expected ones; the two dashed lines show the $\pm 2.8\sigma$ range.

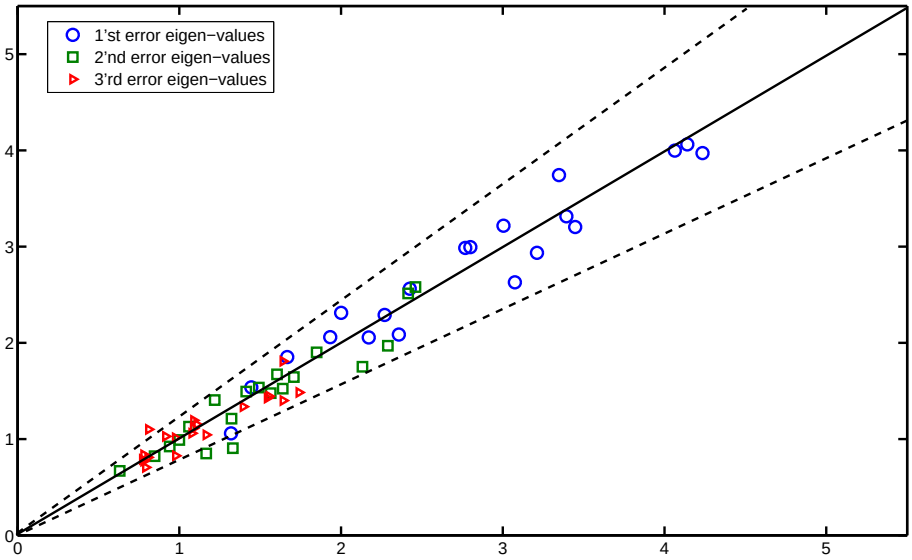

Figure 3: Apodemus data (85×20; as in Figs. 6-7): error eigen-values estimated using the Monte-Carlo data (where mean shape, eigen-vectors, and measurement covariances are identical to the 5-component model which generated the simulated data) against the expected ones; the two dashed lines show the $\pm 2.8\sigma$ range.

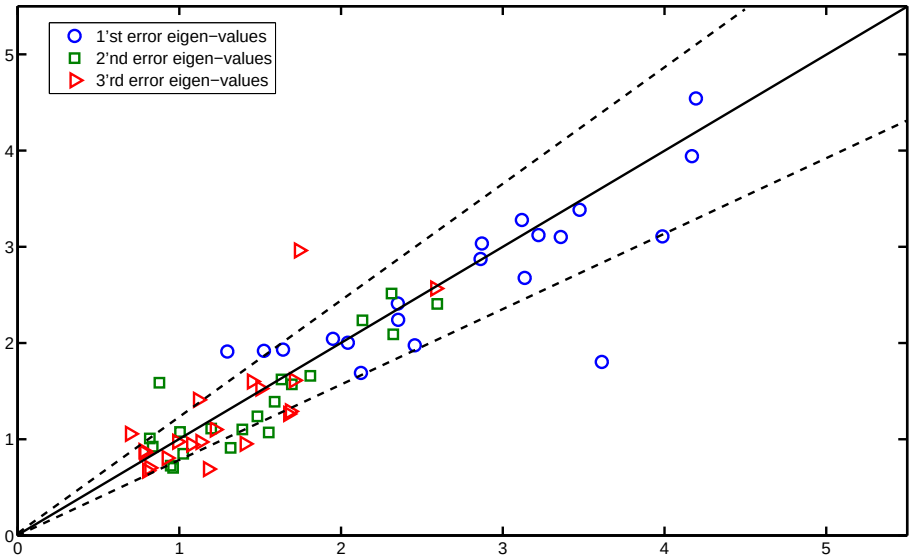

Figure 4: Original Apodemus data (87×20): error eigen-values estimated using the Monte-Carlo data against the expected ones which were used when generating the simulated data; independent models; using 5 model components; the two dashed lines show the $\pm 2.8\sigma$ range.

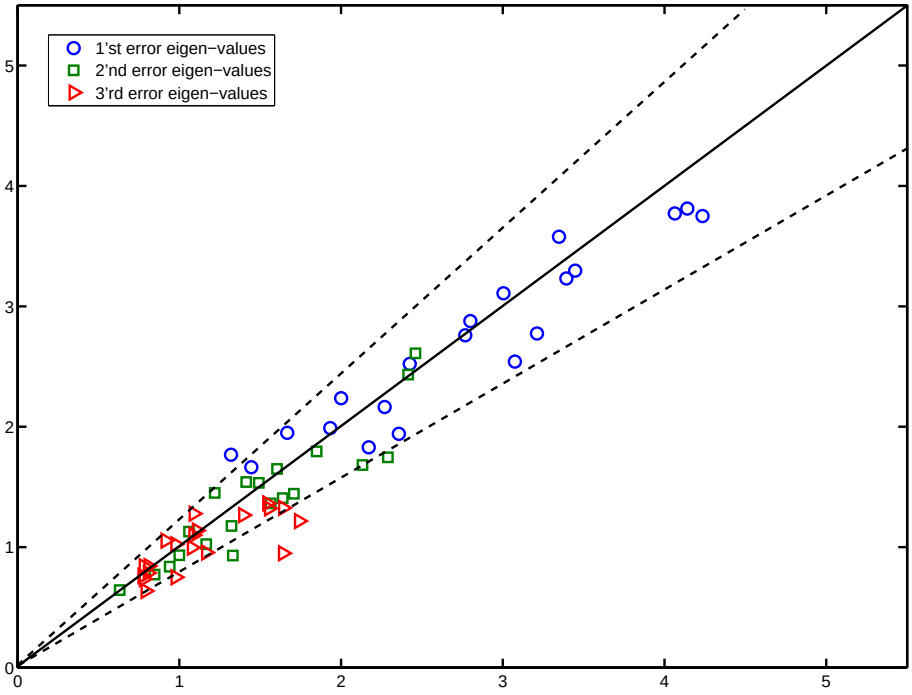

Figure 5: Apodemus data (85×20; as in Figs. 6-7): error eigen-values estimated using the Monte-Carlo data against the expected ones which were used when generating the simulated data; independent models; using 5 model components; the two dashed lines show the $\pm 2.8\sigma$ range.

Fig. 6 shows the aligned data, each figure consists of three projection planes for the purpose of displaying 3D results. These are the xy (bottom-right), xz (top-right) and zy (bottom-left) planes. In order to provide the quantitate results for the covariance estimates displayed here, in Table 2, we list the values of the elements of each

3×3 covariance matrix corresponding to each landmark.

In Fig. 7, we show the anisotropic error bars computed using the eigen vectors and values of the 3x3 covariance matrices. All error bars are rescaled for visualisation purposes (see captions). Error bars for each landmark show the extent of an elliptical (non-isotropic) distribution around the corresponding point in the mean shape. Such distributions estimated using our method show exactly why we cannot assume isotropic distributions for the data as assumed in Procrustes.

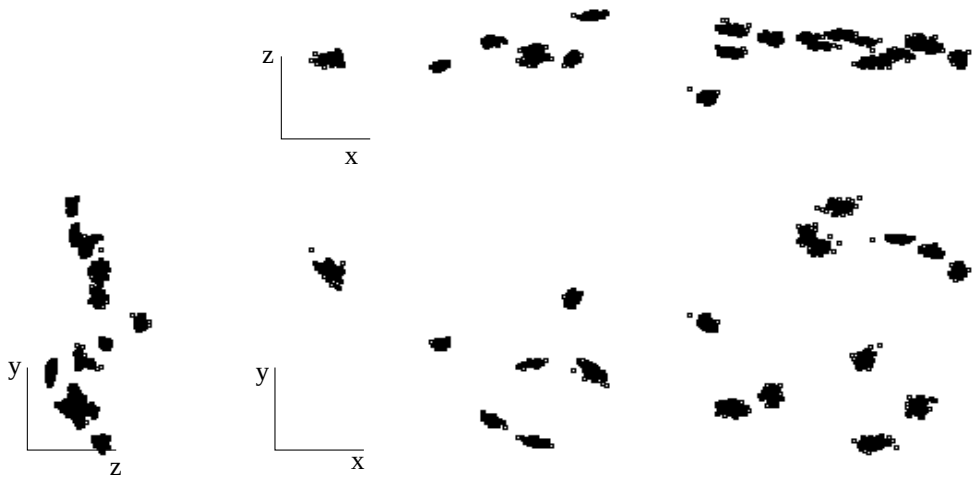

Figure 6: Apodemus mouse mandible data: 85 samples, 20 landmarks (where 2 samples including outliers removed from the original data set); result of data alignment using our covariance-based method. Projected for display purposes on 2D planes, xy (bottom-right), xz (top-right) and zy (bottom-left) planes.

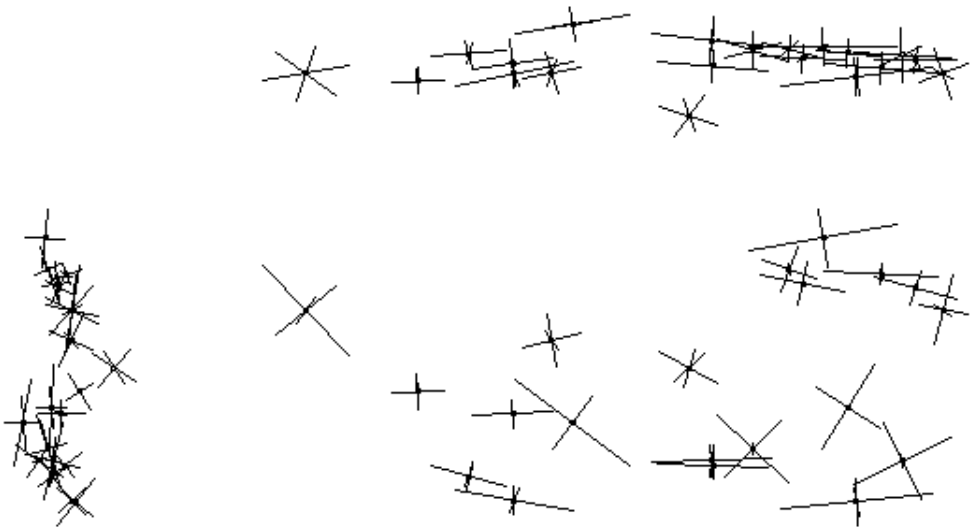

Figure 7: Apodemus mouse 3D data: error bars ($\times 20$) using our covariance-based method (5-component model) showing amount of error in 3 orthogonal directions for each landmark (corresponding to the 3 dimensions of the data); displayed as in Figure 6. above.

Summary

Starting from a 2D shape analysis system which combines linear model construction and iterative shape alignment, extension to the 3D case is in general straight forward, the 2D shape vectors become 3D and the 2x2 anisotropic measurement covariances become 3x3 matrices. The only complication involves the introduction of the two new rotation parameters required to define a 3D rotation. We have done this here using a mechanism which generalises the 2D case of rotation about the viewing axis, by adding two new degrees of freedom associated with rotation

sample	C_{xx}	C_{xy}	C_{xz}	C_{yx}	C_{yy}	C_{yz}	C_{zx}	C_{zy}	C_{zz}
1	8.51949	3.22594	0.24455	3.22594	8.55357	-1.61503	0.24455	-1.61503	3.88968
2	2.08567	-0.00376	-0.04309	-0.00376	1.15918	0.29724	-0.04309	0.29724	0.91916
3	5.07934	-0.15885	-0.46566	-0.15885	0.61432	0.03121	-0.46566	0.03121	1.83603
4	2.81480	-0.15527	-0.28369	-0.15527	2.57364	-0.30391	-0.28369	-0.30391	1.96222
5	3.36557	0.55763	0.18626	0.55763	2.47538	0.44409	0.18626	0.44409	2.41454
6	6.55171	1.20538	0.49769	1.20538	6.04394	1.52578	0.49769	1.52578	1.66256
7	16.70790	-2.47641	-0.00234	-2.47641	3.11547	-0.11302	-0.00234	-0.11302	1.16999
8	2.66613	0.16219	0.27946	0.16219	1.88294	0.51359	0.27946	0.51359	0.82372
9	5.70345	0.83284	0.20853	0.83284	1.63801	0.14386	0.20853	0.14386	0.63115
10	10.21184	0.54180	0.81767	0.54180	0.48026	-0.09692	0.81767	-0.09692	0.85543
11	5.21407	1.19448	-0.01019	1.19448	1.36582	-0.20211	-0.01019	-0.20211	0.74703
12	2.36000	-0.43249	0.10231	-0.43249	3.86169	-0.17606	0.10231	-0.17606	2.38827
13	5.41258	-1.40562	0.37882	-1.40562	6.76309	-0.11885	0.37882	-0.11885	0.65632
14	8.40056	-1.28205	0.01435	-1.28205	6.29284	-0.77092	0.01435	-0.77092	2.57933
15	17.56383	-1.55132	-1.85050	-1.55132	2.47527	-0.28031	-1.85050	-0.28031	2.33656
16	11.09392	-0.32074	0.96195	-0.32074	1.62217	0.53679	0.96195	0.53679	2.16566
17	9.39402	0.26910	0.66831	0.26910	0.92324	-0.31938	0.66831	-0.31938	1.15230
18	10.80942	1.73403	-1.97725	1.73403	1.40466	-0.25635	-1.97725	-0.25635	1.48582
19	4.42357	0.97871	-0.23943	0.97871	1.20148	-0.03388	-0.23943	-0.03388	0.92386
20	11.54245	6.21399	-1.55747	6.21399	8.15980	-1.01520	-1.55747	-1.01520	1.18590

Table 2: The 9 elements of the 3×3 covariance matrices corresponding to the 20 landmarks (rows) of the Apodemus mouse data with 85 samples (5-component model); see Fig. 7.

about the vertical and horizontal axes. These degrees of freedom now generate additional associated biases in covariance estimation when using the residuals observed following Likelihood based model alignment. This bias can be corrected using the method used previously, based upon the associated linearised parameter vectors.

Tests with representative data have shown that the 3D version of the analysis software replicates the statistical behaviour of the previous 2D methods. In particular, the estimation of anisotropic error covariances is demonstrated to be unbiased and within the sampling limits of accuracy expected, once outlier have been identified and removed.

In addition, this data set indicates that the upper bound of 3D landmark repeatability for 3D mandible data is generally between 3-5 pixels, and also that outlier datasets may be present following even careful manual mark-up at the level of 2-3%. Our analysis approach provides the ideal mechanism for not only quantifying the repeatability of mark-up methodology (either manual or automatic) but also identifying possible outlier data. Removal of such data would be expected to improve the stability of subsequent linear models (as illustrated here using Monte-Carlo).

The methods described in this document will be made available via the automatic 3D landmarking tool, as a system for quality assessment and validation of output data.